Available online at www.sciencedirect.com
ScienceDirect
Tetrahedron Letters 49 (2008) 3582–3587
Tetrahedron Letters

Novel cyclopenta[*def*]phenanthrene based blue emitting oligomers for OLEDs

Suhee Song [a], Youngeup Jin [a], Kwanghyun Kim [b], Sun Hee Kim [c], Yoon Bo Shim [a], Kwanghee Lee [c], Hongsuk Suh [a,*]

[a] *Department of Chemistry, and Chemistry Institute for Functional Materials, Pusan National University, Busan 609-735, Republic of Korea*
[b] *LG Electronics Incorporated, Kumi, Kyungbuk, 730-030, Republic of Korea*
[c] *Department of Materials Science and Engineering, Gwangju Institute of Science and Technology, Gwangju 500-712, Republic of Korea*

Received 23 February 2008; revised 31 March 2008; accepted 3 April 2008
Available online 7 April 2008

Abstract

Novel blue emitters, oligo-MCPPs (tri-MCPP, tetra-MCPP, and penta-MCPP), have been synthesized and characterized. The introduction of cyclopenta[*def*]phenanthrene (CPP) units into the structure of oligo-MCPPs gave LEDs with high efficiency and pure blue emission. UV–visible absorption spectra of the thin films of these compounds appear at 333–354 nm, and their maximum PL emission at 416–447 nm. Multilayer organic EL devices with oligo-MCPPs as an emitting layer showed the turn-on voltage of about 4.8 V, the maximum brightness of 1076 cd/m^2 (at 8.2 V), the maximum luminescence efficiency of 0.81 cd/A, and the CIE coordinates of (0.17, 0.14) with blue color.

Keywords: OLEDs; CPP; Blue emission; Oligomers

Organic light-emitting diodes (OLEDs) have been investigated for the intensive subject in recent years due to their applications in displays. For the commercial application of the active matrix full color displays with OLEDs, much effort has been directed toward the improvement of the materials and devices.[1–5] In all these applications, good blue-emitting materials and devices have been essential and efforts continue toward improving their characteristics.[6,7] Three basic colors, red, green, and blue, are needed for a full-color display. Compared with green-emitting devices for full-color applications, the electroluminescence (EL) characteristics of blue- and red-emitting devices need to be improved for efficiency and color purity. Nevertheless, owing to its intrinsic characteristic of having a wide band gap, it is much more difficult to produce a blue emission material.[8] Even though there are many reports about blue OLEDs, only a limited number of materials provide appropriate brightness and stability[9] with much recent interest being paid to fluorene-based small molecules and polymers as efficient blue emitters.[10,11]

Conjugated oligomers with low molecular weights are characterized by the ease of purification, the absence of chain defects, and the structural uniformity into thin films. As compared with polymers, oligomers generally have more expected and reproducible properties that are amenable to optimization through molecular engineering. Nevertheless, it is highly desirable to provide oligomers with a high glass transition temperature (T_g) and superior morphological stability against crystallization.[12] Vacuum deposition of conjugated organic oligomers as thin film was applied for multiple-layer OLEDs, and better efficiency of the device can be accomplished through proper choice of electron- and hole-transport materials.

We previously reported on the synthesis and properties of new EL polymers utilizing a new backbone, poly(2,6-(4,4-bis-(2-ethylhexyl)-4*H*-cyclopenta-[*def*]phenanthrene))

* Corresponding author. Tel.: +82 51 510 2203; fax: +82 51 516 7421.
E-mail address: hssuh@pusan.ac.kr (H. Suh).

0040-4039/$ - see front matter © 2008 Elsevier Ltd. All rights reserved.
doi:10.1016/j.tetlet.2008.04.015

(PCPP) with stabilized pure blue emission.[13,14] A recent work has pointed out the progress in the synthesis of high band gap materials based on the phenanthrene building block.[14–16] EL spectra of PCPP do not show any peak in the long wavelength region corresponding to keto defect sites or aggregates/excimers even after annealing the device for 18 hrs in air or operation of the device for 40 min. Therefore, efforts should be made to incorporate this new 4*H*-cyclopenta[*def*]phenanthrene (CPP) unit in a small molecule for LED to enhance the morphologic stability for highly efficient blue-light-emission. Herein, we report the syntheses and characterizations of efficient blue-light-emitting materials, oligo-MCPPs (tri-MCPP, tetra-MCPP, and penta-MCPP). The Yamamoto and Suzuki coupling reactions were employed to prepare oligo-MCPPs in high yields. These CPP-based conjugated small molecules showed good thermal stability and optical and electrochemical properties with potential for the display technologies.

The general synthetic routes toward the monomers and oligomers are outlined in Scheme 1. In the first step, 4*H*-cyclopenta[*def*]phenanthrene (**1**) was alkylated using CH_3I in DMSO and 50% aqueous NaOH to obtain 4,4-dimethyl-4*H*-cyclopenta[*def*]phenanthrene (**2**), which was hydrogen-nated using Pd/C to generate 4,4-dimethyl-8,9-dihydro-4*H*-cyclopenta[*def*]phenanthrene (**3**). Mono-bromination of compound **3** with N-bromosuccinimide (NBS) afforded 2-bromo-4,4-dimethyl-8,9-dihydro-4*H*-cyclopenta[*def*]phenan-threne (**4**). Alumina-supported copper (II) bromide[17] was used for the dibromination to provide 2,6-dibromo-4,4-dimethyl-8,9-dihydro-4*H*-cyclopenta[*def*]phenanthrene (**5**). Compounds **4** and **5** were dehydrogenated by bromine and carbon disulfide to provide 2-bromo-4,4-dimethyl-4*H*-cyclo-penta[*def*]phenanthrene (**6**) and 2,6-dibromo-4,4-dimethyl-4*H*-cyclopenta-[*def*]phenanthrene (**7**), which afforded 2-(4,4-dimethyl-4*H*-cyclopenta[*def*]phenanthren-2-yl)-4,4,5,5-tetra-methyl-1,3,2-dioxaborolane (**8**) and 2-[4,4-dimethyl-6-(4,4,5,5-tetramethyl-1,3,2-dioxaborolan-2-yl)-4*H*-cyclopenta-[*def*]phenanthren-2-yl]-4,4,5,5-tetra-methyl-1,3,2-dioxaboro-lane (**9**) using bis(pinacolato)diboron, catalytic amounts of $Pd(dppf)Cl_2$, and potassium acetate in DMF. Suzuki

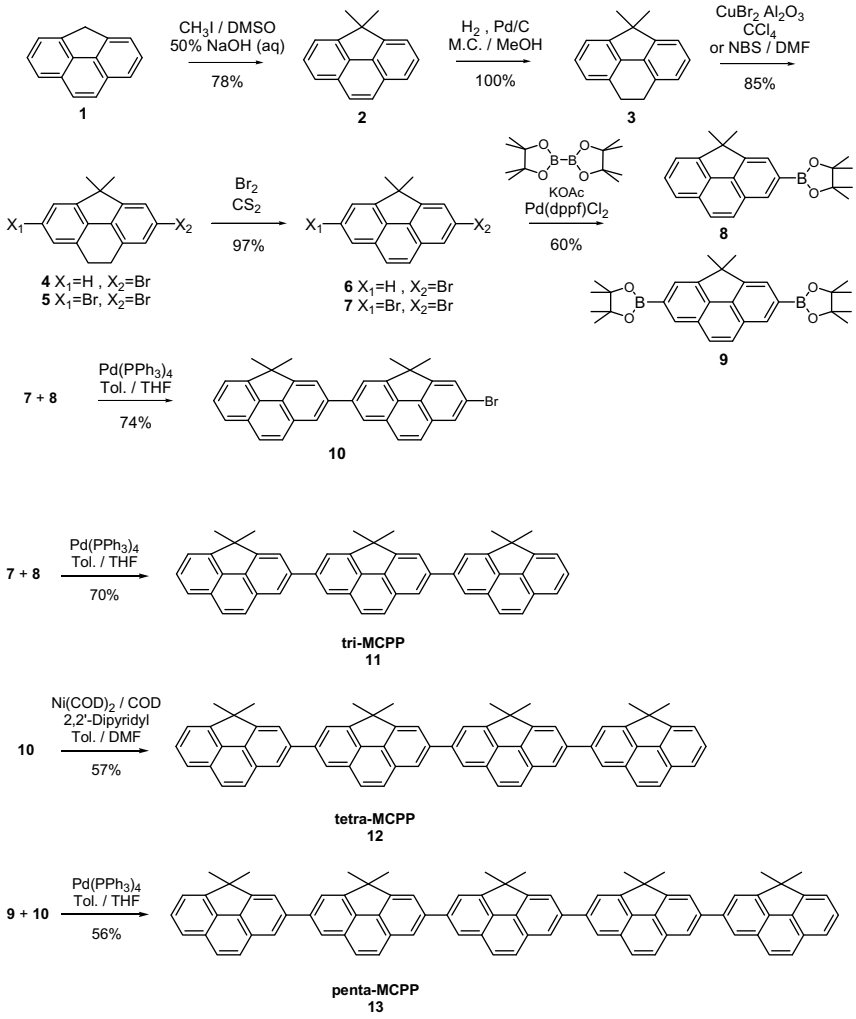

Scheme 1. Synthetic routes for monomer of tri-MCPP, tetra-MCPP, and penta-MCPP.

coupling[18] was employed for the synthesis of 7-bromo-9,9′,9′-tetramethyl-2,2′-bi-4*H*-cyclopenta[*def*]phenanthrene (**10**) using compound **7**, compound **8**, $Pd(PPh_3)_4$, and K_2CO_3 in dilute DMF. Tri-MCPP (**11**)[19] was synthesized using the same condition as compound **10** in dense solution. Tetra-MCPP (**12**)[20] was synthesized by Yamamoto coupling[21] of compound **10** using the bis(1,5-cyclooctadiene) nickel(0) (Ni(COD)) catalyst, 2,2′-dipyridyl, and cyclooctadiene. Suzuki coupling was performed for the synthesis of penta-MCPP (**13**)[22] using compound **9** and compound **10**.

The thermal properties of tri-MCPP, tetra-MCPP and penta-MCPP were evaluated by differential scanning calorimetry (DSC) and thermo gravimetric analysis (TGA) in nitrogen (Table 1). The differential scanning calorimetry analysis was performed under a nitrogen atmosphere (50 mL/min) on a DSC 822 at heating rates of 10 °C/min. Thermogravimetric analysis was performed with a Dupont 951 TGA instrument in a nitrogen atmosphere at a heating rate of 10 °C/min to 800 °C. The TGA results clearly indicated that all the oligomers have good thermal stability. Their decomposition temperatures (T_d), which correspond to a 5% weight loss upon heating during TGA, are around 395 °C, 510 °C, and 514 °C for tri-MCPP, tetra-MCPP, and penta-MCPP, respectively. It was also interesting to note that the T_d increased by about 115 °C from tri-MCPP to tetra-MCPP, but further increasing the length of the oligomer (tetra-MCPP–penta-MCPP) did not produce any additional increase in T_d. DSC was performed in the temperature range from 30 to 450 °C to show that the glass transition temperatures (T_g) of tri-MCPP, tetra-MCPP, and penta-MCPP occur at 122, 156, and 187 °C, respectively. The DSC curve of tetra-MCPP showed a crystallizing peak around 341 °C followed by a melting peak around 377 °C. No transitions related to crystalline structures were observed for tri-MCPP and penta-MCPP. Crystalline melting peaks (T_m) of the oligo-MCPPs increased from 340 to 412 °C as the longer length of the oligo-MCPP increased. The increase in T_g, and T_m with the progression from tri-MCPP to penta-MCPP can be attributed to the increase of the CPP units in the materials. Consequently, oligo-MCPPs are able to form homogeneous and stable amorphous films by thermal evaporation, which is a basic requirement for the materials to be used as hosts in OLEDs.

The UV–vis absorption spectra and photoluminescence spectra of tri-MCPP, tetra-MCPP, and penta-MCPP as THF solution and in thin film are presented in Figure 1. All the oligomers displayed intense π–π* absorption bands

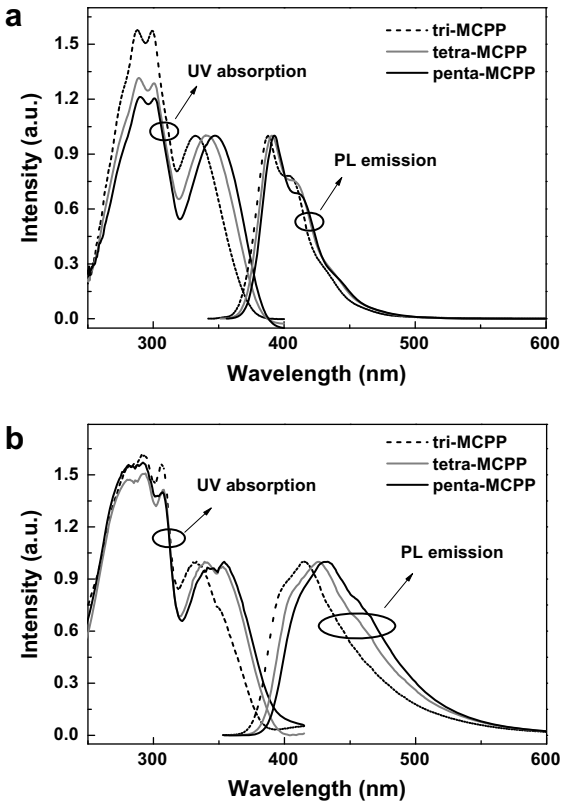

Fig. 1. UV–vis absorption and photoluminescence emission spectra of tri-MCPP, tetra-MCPP, and penta-MCPP in THF solution (a) and in thin film (b).

Table 1
Thermal, electrochemical, and optical properties of tri-MCPP, tetra-MCPP, and penta-MCPP

Materials	T_g[a]/T_m/T_d[b] (°C)	HOMO[c] (eV)	LUMO[d] (eV)	Band gap[e] (eV)	Solution				Film			
					λ_{abs} (nm)	λ_{PL} (nm)	fwhm[f] of PL	QE_{PL} (%)	λ_{abs} (nm)	λ_{PL} (nm)	fwhm[f] of PL	QE_{PL} (%)
Tri-MCPP	122/340/395	5.69	2.44	3.25	332	388	39	34.8	333	415	65	62.1
Tetra-MCPP	156/377/510	5.64	2.49	3.15	340	391	41	59.8	353	426	76	83.3
Penta-MCPP	187/412/514	5.62	2.48	3.14	347	393	40	97.7	354	433	79	92.9

[a] Glass transition temperature measured by DSC under N_2.
[b] Onset decomposition temperature (5% weight loss) measured by TGA under N_2.
[c] The HOMO energy levels of organic thin films were measured using atmospheric low-energy photoelectron spectrometer Riken-Keiki AC-2.
[d] Calculated from the HOMO energy levels and E_g.
[e] Energy band gap was estimated from the onset wavelength of the optical absorption in solid state.
[f] Full width at half-maximum of PL spectra.

both in solution and as films. Oligo-MCPPs exhibit maximum absorption peaks from 332 to 347 nm in solution, which were red-shifted owing to increasing conjugation length. The absorption spectra (333–354 nm) in the thin solid state for each oligomer were similar as compared to those in solution. The PL spectra of oligo-MCPPs in THF solution exhibit maxima at 388–393 nm. The PL spectrum of penta-MCPP in THF is red-shifted about 5 nm as compared to that of tri-MCPP. The PL spectra of oligo-MCPPs in thin films exhibit maxima at 415–433 nm. The PL spectrum of penta-MCPP in thin film is red-shifted about 30 nm compared to that of tri-CPP. In the case of a solid thin film, the maximum emission peaks of oligo-MCPPs are red-shifted over 30–40 nm, and full width at half-maximum (fwhm) of PL spectra are increased over 26–39 nm, as compared to the case of solution, indicating that the inter-chain interaction of oligo-MCPPs, which can be attributed to the π–π^* transitions of conjugated backbone, increased the planarity of the materials in the solid state.

Listed in Table 1 are the PL efficiencies of the oligomers in solution and as films. Quantum yields (Φ_{PL}) of tri-, tetra-, and penta-MCPP in chloroform with 9,10-diphenylanthracene as the standard ($\Phi_{PL} = 0.91$ in ethanol) are 34.8%, 59.8%, and 97.7%, respectively. The Φ_{PL} value increases significantly with the conjugation lengths of the oligomers. Quantum yields of the films were determined in an integrating sphere at room temperature in air, relative to a thin film of $\sim 10^{-3}$ M 9,10-diphenylanthracene in poly(methyl methacrylate) (PMMA) as the standard ($\Phi_{PL} = 0.83$). The PL quantum yield of penta-MCPP using a 10 wt % film of emitter in PMMA was 92.9%, lower than its solution equivalent due most likely to quenching or decreasing of aggregation effects. Quantum yield of tetra-MCPP ($\Phi_{PL} = 0.83$) and tri-MCPP ($\Phi_{PL} = 0.62$) could be higher than their solution equivalents, due to regular packing by thermal deposition in solid state. This property makes these materials excellent candidates for the use in OLEDs.

The absorption onset wavelength of tri-MCPP was 382 nm, corresponding to a band gap of 3.25 eV, which tetra-MCPP was 394 nm, corresponding to a band gap of 3.15 eV, and that of penta-MCPP was 395 nm, corresponding to a band gap of 3.14 eV. Increasing the conjugated length of the oligo-MCPPs from three to five CPP units resulted in lowering the band gap from 3.27 to 3.18 eV. The HOMO levels for the oligomers were measured to be between −5.62 and −5.69 eV. Increasing the conjugated length of the oligo-MCPP leads to increased HOMO levels. The LUMO levels were calculated from the values of the band gap and the HOMO energy level to be between −2.44 and −2.49 eV. By using the estimated energy levels of oligo-MCPPs, the materials for hole-transport layer (HTL), hole-blocking layer (HBL), and electron-transport layer (ETL) were chosen for the increase of both hole and electron affinities and the improvement of charge injection of the device. *N*,*N*′-Bis(naphthalen-1-yl)-*N*,*N*′-bis(phenyl)benzidine (NPD) as HTL and 8-hydroxyquinoline aluminum (Alq_3) as ETL were used in all of the device

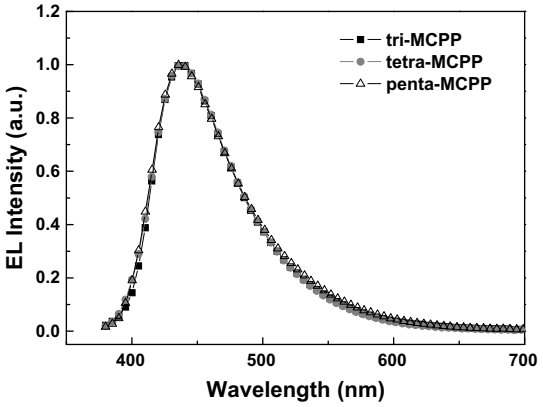

Fig. 2. Electroluminescence spectra of OLEDs with configurations of ITO (150 nm)/NPD (40 nm)/oligo-MCPPs (30 nm)/BAlq (10 nm)/Alq_3 (20 nm)/LiF (0.5 nm)/Al (100 nm).

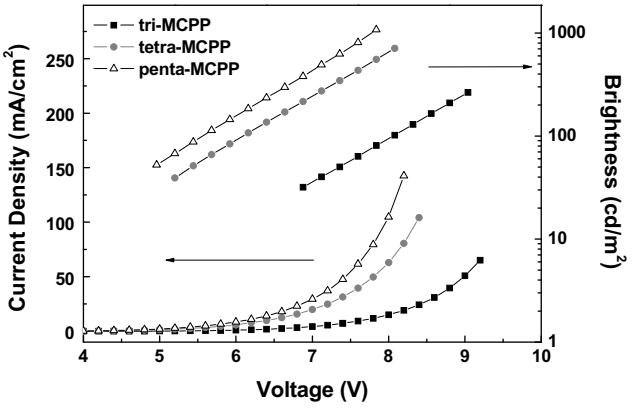

Fig. 3. Current density–voltage–luminescence (*J*–*V*–*L*) characteristics of OLEDs with configurations of ITO (150 nm)/NPD (40 nm)/oligo-MCPPs (30 nm)/BAlq (10 nm)/Alq_3 (20 nm)/LiF (0.5 nm)/Al (100 nm).

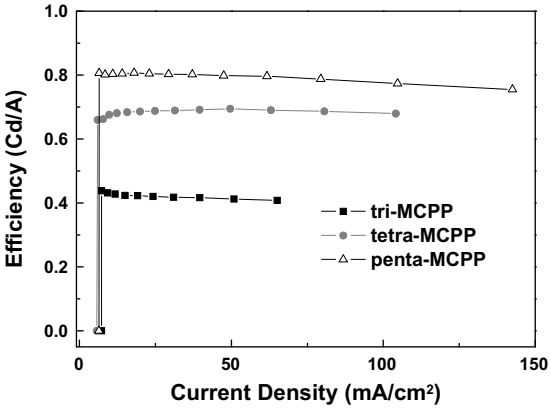

Fig. 4. Efficiency characteristics of OLEDs with configurations of ITO (150 nm)/NPD (40 nm)/oligo-MCPPs (30 nm)/BAlq (10 nm)/Alq_3 (20 nm)/LiF (0.5 nm)/Al (100 nm).

Table 2
Device performance characteristics of tri-MCPP, tetra-MCPP, and penta-MCPP

	EL λ_{max} (nm)	fwhm[a] of EL	Turn-on voltage (V)	Current density (mA/cm^2)	Brightness[b] (cd/m^2)	Efficiency[c] (cd/A)	CIE (x, y)[d]
Tri-MCPP	438	74	6.2	65.1	276.4	0.42	(0.17, 0.13)
Tetra-MCPP	438	74	5	104.2	708.1	0.69	(0.16, 0.13)
Penta-MCPP	438	74	4.8	142.6	1076	0.81	(0.17, 0.14)

[a] Full width at half-maximum of EL spectra.
[b] Measured under the condition of maximum brightness.
[c] Maximum luminescence efficiency.
[d] Calculated from the EL spectra at 8 V.

fabrications. Bis(2-methyl-8-quinolinolato)-4-(phenyl-phenolato)aluminum-(III) (BAlq) as HBL was also applied.

The multi-layered OLEDs with the configuration of ITO (150 nm)/NPD (40 nm)/oligo-MCPPs(30 nm)/BAlq (10 nm)/Alq_3 (20 nm)/LiF (0.5 nm)/Al (100 nm) were fabricated to investigate the electroluminescent properties and the current–voltage–luminescence characteristics of the oligo-MCPPs. To decrease the operating voltage and smooth the surface roughness of ITO, NPD as HTL was deposited by thermal evaporation. Deposited on top of the NPD layer by thermal evaporation were oligo-MCPPs as the emissive layer, BAlq as HBL, Alq_3 as ETL, LiF as electron injection layer and Al as cathode.

Figure 2 shows the EL spectra of the devices with the configuration of ITO/NPD/oligo-MCPPs/BAlq/Alq_3/LiF/Al. The effects of the presence of BAlq as the hole blocking layers are illustrated. All the oligo-MCPPs display a deep-blue EL emission spectra at 438 nm like that of PCPP at 433 nm, indicating that the oligomers of CPP have same conjugated length as the polymers after spin-casting films.

The performance of the devices is illustrated in Figure 3. It can be seen that all the devices fabricated using the oligo-MCPPs have a low turn-on voltage (voltage at 1 mA/cm^2), which decreased from 6.2 V to 4.8 V. In assessing the performance of these three devices, it is interpreted that the lower turn on voltage observed for the penta-MCPP cannot only be attributed to a conjugation effect but to the better emitting properties of the penta-MCPP probably deriving form the increased extensive conjugation. It would appear that the device using penta-MCPP is the best, with the highest luminance of 1076 cd/m^2 at 8.2 V. The maximum brightness of tri-MCPP and tetra-MCPP was 276.4 and 708.1 cd/m^2, respectively. The EL efficiency of oligo-MCPPs, according to the efficiency versus current density plot, increased as shown in Figure 4. The luminous efficiencies of the devices are 0.42 cd/A at 31 cd/m^2 for tri-MCPP, 0.69 cd/A at 63 cd/m^2 for tetra-MCPP, and 0.81 cd/A at 18 cd/m^2 for penta-MCPP. Compared with the luminous efficiencies of other colors, these values are not high. It should be noted that the emissions of these devices are deep blue in color, as indicated by the very low y values of the Commission Internationale de l'Eclairage (CIE) color coordinates.[23] As shown in Table 2, the CIE color coordinates of the emission of tri-MCPP, tetra-MCPP, and penta-MCPP are (0.17, 0.13), (0.16, 0.13), and (0.17, 0.14), respectively, at approximately 8 V. These are quite close to that of the National Television System Committee (NTSC) standard blue (0.14, 0.08). Herein, we conclude that the CPP unit, which is a new conjugated emitting segment, can be applied to many kinds of highly efficient materials as blue emissive layers in OLEDs.

In conclusion, we have designed and synthesized novel blue emitter oligo-MCPPs to achieve high efficiency and pure blue emission. Thermal analysis of these revealed their high thermal stability. Decomposition temperatures were around 395 °C for tri-MCPP and over 500 °C for tetra-MCPP and penta-MCPP. These oligomers displayed a bright, deep-blue fluorescence in both the solution and the solid state. High PL quantum efficiencies have been achieved in the oligomers where the oligomers contain three to five CPP units. The multi-layered OLEDs with the configuration of ITO/NPD/oligo-MCPPs/BAlq/Alq_3/LiF/Al were fabricated to investigate the electroluminescent properties and the current–voltage–luminescence characteristics of the compounds. The EL spectra of oligo-MCPPs showed maximum peaks around 438 nm. The device of penta-MCPP with the configuration of ITO/NPD/penta-MCPP/BAlq/Alq_3/LiF/Al showed the turn-on voltage of about 4.8 V, the maximum brightness of 1076 cd/m^2 (at 8.2 V), the maximum luminescence efficiency of 0.81 cd/A, and CIE coordinates of 0.17 and 0.14.

Acknowledgment

This work was supported by the Ministry of Information and Communications, Korea, under the Information Technology Research Center (ITRC) Support Program.

References and notes

1. Caruso, F.; Spasova, M.; Maceira, V. S.; Marzan, M. L. *Adv. Mater.* **2001**, *13*, 1090.
2. Zhao, H.; Tanjutco, C.; Thayumanavan, S. *Tetrahedron Lett.* **2001**, *42*, 4421.
3. Li, Z. H.; Wong, M. S.; Fukutani, H.; Tao, Y. *Chem. Mater.* **2005**, *17*, 5032.

4. Grisorio, R.; Dell'Aquila, A.; Romanazzi, G.; Suranna, G. P.; Mastrorilli, P.; Cosma, P.; Acierno, D.; Amendola, E.; Ciccarellaf, G.; Nobile, C. F. *Tetrahedron* **2006**, *62*, 627.
5. Leung, A. C. W.; MacLachlan, M. J. *J. Mater. Chem.* **2007**, *17*, 1923.
6. Wu, C. C.; Lin, Y. T.; Wong, K. T.; Chen, R. T.; Chien, Y. Y. *Adv. Mater.* **2004**, *16*, 61.
7. Promarak, V.; Saengsuwan, S.; Jungsuttiwong, S.; Sudyoadsuk, T.; Keawin, T. *Tetrahedron Lett.* **2007**, *48*, 89.
8. Kim, Y. H.; Jeong, H. C.; Kim, S. H.; Yang, K.; Kwon, S. K. *Adv. Funct. Mater.* **2005**, *15*, 1799.
9. Li, Y.; Fung, M. K.; Xie, Z.; Lee, S. T.; Hung, L. S.; Shi, J. *Adv. Mater.* **2004**, *14*, 1317.
10. Redecker, M.; Bradley, D. D. C.; Inbasekaran, M.; Woo, E. P. *Appl. Phys. Lett.* **1998**, *73*, 1565.
11. Wong, K. T.; Chien, Y. Y.; Chen, R. T.; Wang, C. F.; Lin, Y. T.; Chiang, H. H.; Hsieh, P. Y.; Wu, C. C.; Chou, C. H.; Su, Y. O.; Lee, G. H.; Peng, S. M. *J. Am. Chem. Soc.* **2002**, *124*, 11576.
12. Katsis, D.; Geng, Y. H.; Ou, J. J.; Culligan, S. W.; Trjkovska, A.; Chen, S. H.; Rothberg, L. J. *Chem. Mater.* **2002**, *14*, 1332.
13. Park, S. H.; Jin, Y.; Kim, J. Y.; Kim, S. H.; Kim, J.; Suh, H.; Lee, K. *Adv. Funct. Mater.* **2007**, *17*, 3063.
14. Suh, H.; Jin, Y.; Park, S. H.; Kim, D.; Kim, J.; Kim, C.; Kim, J. Y.; Lee, K. *Macromolecules* **2005**, *38*, 6285.
15. He, B.; Tian, H.; Geng, Y.; Wang, F.; Mullen, K. *Ogr. Lett.* **2008**, *10*, 773.
16. Grisorio, R.; Suranna, G. P.; Mastrorilli, P.; Nobile, C. F. *Org. Lett.* **2007**, *9*, 3149.
17. Mitsuo, K.; Hiroaki, S.; Suehiko, Y. *J. Org. Chem.* **1988**, *53*, 2093.
18. Miyaura, N.; Yanagi, T.; Suzuki, A. *Synth. Commun.* **1981**, *11*, 513.
19. R_f 0.35 (SiO_2, dichloromethane/*n*-hexane = 1:10); ^{1}H NMR (300 MHz, $CDCl_3$) δ (ppm) 1.81 (s, 12H), 1.89 (s, 6H), 7.63 (dd, 2H, $J = 0.8$ and 6.9 Hz), 7.69 (t, 2H, $J = 4.1$ Hz), 7.85 (dd, 2H, $J = 0.8$ and 7.7 Hz), 7.95 (s, 2H), 7,97 (s, 2H), 7.99 (dd, 4H, $J = 1.1$ and 3.3 Hz), 8.02 (s, 2H), 8.19 (d, 2H, $J = 1.7$ Hz), 8.20 (s, 2H); ^{13}C NMR (300 MHz, $CDCl_3$) δ (ppm) 26.54, 26.67, 50.92, 51.21, 118.80, 119.72, 119.87, 122.98, 123.05, 123.11, 125.58, 125.95, 126.08, 127.67, 128.05, 128.06, 128.07, 134.57, 134.72, 135.38, 143.37, 143.45, 152.40, 152.71, 152.94; HRMS (*m*/*z* , EI^+) calcd for $C_{51}H_{38}$ 650.2974, found 650.2975.
20. R_f 0.3 (SiO_2, dichloromethane/*n*-hexane = 1:8); ^{1}H NMR (300 MHz, $CDCl_3$) δ (ppm) 1.83 (s, 12H), 1.93 (s, 12H), 7.64 (d, 2H, $J = 6.6$ Hz), 7.70 (t, 2H, $J = 7.6$ Hz), 7.86 (d, 2H, $J = 7.7$ Hz), 7.96 (d, 4H, $J = 5.1$ Hz), 8.02 (d, 6H, $J = 4.7$ Hz), 8.04 (s, 4H), 8.21 (s, 2H), 8.23 (d, 4H, $J = 7.2$ Hz); ^{13}C NMR (300 MHz, $CDCl_3$) δ (ppm) 26.96, 27.09, 51.35, 51.66, 119.23, 120.15, 120.31, 123.42, 123.48, 123.55, 126.01, 126.38, 126.52, 128.10, 128.11, 128.48, 128.51, 128.54, 135.02, 135.03, 135.16, 135.81, 143.80, 143.89, 152.83, 153.14, 153.37, 153.39; HRMS (*m*/*z* , FAB^+) calcd for $C_{68}H_{51}$ 867.3991, found 867.3983.
21. Yamamoto, T.; Morita, A.; Miyazaki, Y.; Maruyama, T.; Wakayama, H.; Zhou, Z. H.; Nakamura, Y.; Kanbara, T.; Sasaki, S.; Kubota, K. *Macromolecules* **1992**, *25*, 1214.
22. R_f 0.38 (SiO_2, dichloromethane/*n*-hexane = 1:3); ^{1}H NMR (300 MHz, $CDCl_3$) δ (ppm) 1.82 (s, 12H), 1.92 (s, 12H), 1.93 (s, 6H), 7.64 (d, 2H, $J = 7.1$ Hz), 7.68 (t, 2H, $J = 6.9$ Hz), 7.86 (d, 2H, $J = 7.7$ Hz), 7.96 (d, 4H, $J = 6.3$ Hz), 8.01 (d, 4H, $J = 4.9$ Hz), 8.04 (s, 10H), 8.20 (s, 2H), 8.21 (s, 2H), 8.24 (s, 4H); ^{13}C NMR (300 MHz, $CDCl_3$) δ (ppm); 26.54, 26.68, 50.93, 51.94, 118.82, 119.73, 119.90, 112.99, 123.04, 123.12, 125.58, 125.96, 126.10, 128.05, 128.08, 128.12, 134.58, 134.61, 124.76, 135.38, 143.38, 143.48, 152.41, 152.73, 152.96, 152.98; HRMS (*m*/*z* , FAB^+) calcd for $C_{85}H_{63}$ 1083.4930, found 1083.4922.
23. Liu, Q. D.; Lu, J.; Ding, J.; Day, M.; Tae, Y.; Barrios, P.; Stupak, J.; Chan, K.; Li, J.; Chi, Y. *Adv. Funct. Mater.* **2007**, *17*, 1028.